Rhodium(I) Complexes of a Chiral Amidophosphine−Phosphinite Chelate. Dinuclear Complexes with Chelating and Bridging Ligands

Nantko Feiken, Paul Pregosin,* and Gerald Trabesinger

Inorganic Chemistry, ETH Zürich, Universitätstrasse 6, CH-8092 Zürich, Switzerland

Received March 17, 1998

Rh(I) complexes of the chiral bidentate ligand (*S*)-*N*-diphenylphosphino-2-diphenylphosphinoxy-3,3,*N*-trimethylbutyramide (**1**) are reported. Two equivalents of **1** react with [RhCl(1,5-COD)]$_2$ slowly in MeOH to afford an isolable unsymmetrical dinuclear complex [(**1**)Rh(μ-Cl)(μ-**1**)Rh(1,5-COD)]Cl (**2**), and the symmetrical dinuclear compound [Rh(μ-Cl)(**1**)]$_2$, which exists in two forms, sym-trans (**3**) and sym-cis (**4**), in solution. In CD_2Cl_2 solution, **2** converts slowly to **3** and **4**. Two-dimensional exchange spectroscopy on **2** reveals an intramolecular and an intermolecular process during the reaction in CD_2Cl_2. A second dinuclear cation, [(**1**)Rh(μ-Cl)(μ-**1**)Rh(**1**)]$^+$ (**6**), containing 3 equiv of **1**, can be prepared from the PF_6 analogue of **2**. [Rh(1,5-COD)(**1**)]OTf (**7a**), [RhCl(PPh_3)(**1**)] (**8**), [Rh(CO)(PPh_3)(**1**)]Cl (**9**), air-sensitive [Rh(**1**)(solvent)$_2$]OTf (**10**), and [RhCl(CNBu^t)(**1**)] (**11**) are reported. The solid-state structures for **3** and **7a** have been determined by X-ray diffraction.

Introduction

Chiral bidentate phosphine auxiliaries play an increasingly important role in enantioselective homogeneous catalysis.[1] Apart from the extremely successful atropisomeric bidentates Binap[2] and Biphep,[3] an ever increasing number of these auxiliaries contain two different donor atoms.[4] Such chelates may contain two tertiary phosphines with different alkyl and/or aryl substituents, e.g., Josiphos,[5] or the donors may be completely different. *P,N*-(oxazoline) chelates[1a,6] have been utilized by Helmchen and Pfaltz, a *P,N*-(quinoline) compound has been studied by Brown and co-workers,[7] and a variety of *P,N*-(pyrazole) types applied by Togni.[8] As we have shown, P,S[9a] and N,S[9b] combinations can also be successfully employed.[9]

A third approach, pioneered by Mortreux[10] and his group, uses a bidentate phosphorus chelate in which the donor atoms are attached to electronegative substituents. Within this class, we have become interested in the P−N, P−O ligand **1** (Ph-t-LANOP). We report here

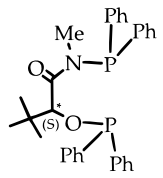

1

some aspects of its Rh(I) chemistry and, particularly, its interesting capability to form dinuclear rhodium complexes containing 2 or 3 equiv of **1**.

Results and Discussion

[(1)Rh (μ-Cl)(μ-1)Rh(1,5-COD]Cl, 2. The reaction of [Rh(μ-Cl)(COD)]$_2$ with 2 equiv of Ph-t-Lanop, **1**, in MeOH proceeds relatively slowly. The major product, **2** (ca 70%), can be separated from the sym-trans and sym-cis isomers of [Rh(μ-Cl)(Ph-t-LANOP)]$_2$, **3** and **4**,

(1) (a) Pfaltz, A. *Acta Chim. Scand.* **1996**, *50*, 189. (b) Trost, B. M.; van Vranken, D. L. *Chem. Rev.* **1996**, *96*, 395. (c) Pfaltz, A. *Acc. Chem. Res.* **1993**, *26*, 339. (d) Hayashi, T. *Catalytic Asymmetic Synthesis*; VCH Publishers: New York, 1993.

(2) Kitamura, M.; Noyori, R. In *Mod. Synth. Meth.* **1989**, *5*, 116. Ohta, T.; Tonomura, Y.; Nozaki, K.; Takaya, H.; Mashima, K. *Organometallics* **1996**, *15*, 1521. Zhang, X.; Uemura, T.; Matsumura, K.; Sayo, N.; Kumobayashi, H.; Takaya, H. *Synlett* **1994**, 501. Kitamura, M.; Tokunaga, M.; Noyori, R. *J. Am. Chem. Soc.* **1993**, *115*, 144. Ohta, T.; Miyake, T.; Seido, N.; Kumobayashi, H.; Akutagawa, S.; Takaya, H. *Tetrahedron Lett.* **1992**, *33*, 635. Mashima, K.; Hino, T.; Takaya, H. *J. Chem. Soc., Dalton Trans* **1992**, 2099. Ohta, T.; Takaya, H.; Noyori, R. *Inorg. Chem.* **1988**, *27*, 566.

(3) Crameri, Y.; Foricher, J.; Hengartner, U.; Jenny, C.; Kienzle, F.; Ramuz, H.; Scalone, M.; Schlageter, M.; Schmid, R.; Wang, S. *Chimia* **1997**, *51*, 303. Schmid, R.; Broger, E. A.; Cereghetti, M.; Crameri, Y.; Foricher, J.; Lalonde, M.; Mueller, R. K.; Scalone, M.; Schoettel, G.; Zutter, U. *Pure Appl. Chem.* **1996**, *68*, 131. Heiser, B.; Broger, E. A.; Crameri, Y. *Tetrahedron: Asymmetry* **1991**, *2*, 51 and references therein.

(4) *Organic Synthesis via Organometallics OSM 5*; Helmchen, G., Dibo, J., Flubacher, D., Wiese. B., Eds.; Vieweg: Braunschweig/Wiesbaden, Germany, 1997.

(5) Togni, A. *Angew. Chem.* **1996**, *108*, 1581. Pregosin, P. S.; Salzmann, R.; Togni, A. *Organometallics* **1995**, *14*, 842. Togni, A.; Breutel, C.; Schnyder, A.; Spindler, F.; Landert, H.; Tijani, A. *J. Am. Chem. Soc.* **1994**, *116*, 4062. Togni, A.; Breutel, C.; Soares, M.; Zanetti, N.; Gerfin, T.; Gramlich, V.; Spindler, F.; Rihs, G. *Inorg. Chim. Acta* **1994**, *222*, 213.

(6) von Matt, Loiseleur, O.; Koch, G.; Pfaltz, A.; Lefeber, C.; Feucht, T. Helmchen, G. *Tetrahedron: Asymmetry* **1994**, *5*, 573.

(7) Brown, J. M. *Chem. Soc. Rev.* **1993**, 25. Brown, J. M.; Hulmes, D. I.; Guiry, P. J. *Tetrahedron* **1994**, *50*, 4493. Brown, J. M.; Lloyd-Jones, G. C. *J. Am. Chem. Soc.* **1994**, *116*, 866.

(8) Togni, A.; Burckhardt, U.; Gramlich, V.; Pregosin, P.; Salzmann, R. *J. Am. Chem. Soc.* **1996**, *118*, 1031. Schnyder, A.; Togni, A.; Wiesli, U. *Organometallics* **1997**, *16*, 255.

(9) (a) Albinati, A.; Pregosin, P. S.; Wick, K. *Organometallics* **1996**, *15*, 2419. Barbaro, P.; Currao, A.; Herrmann, J.; Nesper, R.; Pregosin, P. S.; Salzmann, R. *Organometallics* **1996**, *15*, 1879. (b) Boog-Wick, K.; Pregosin, P. S.; Trabesinger, G. *Organometallics* **1998**, *17*, 3254.

(10) Mortreux, A.; Petit, F.; Buono, G.; Peiffer, G. *Bull. Soc. Chim. Fr.* **1987**, 632. Roucoux, A.; Carpentier, J.; Devocelle, M.; Agboussou, F.; Mortreux, A *SYNLETT* **1995**, 358.

S0276-7333(98)00200-3 CCC: $15.00
Publication on Web 09/12/1998

Scheme 1. Preparation of 2 as Cl and PF_6 Salts

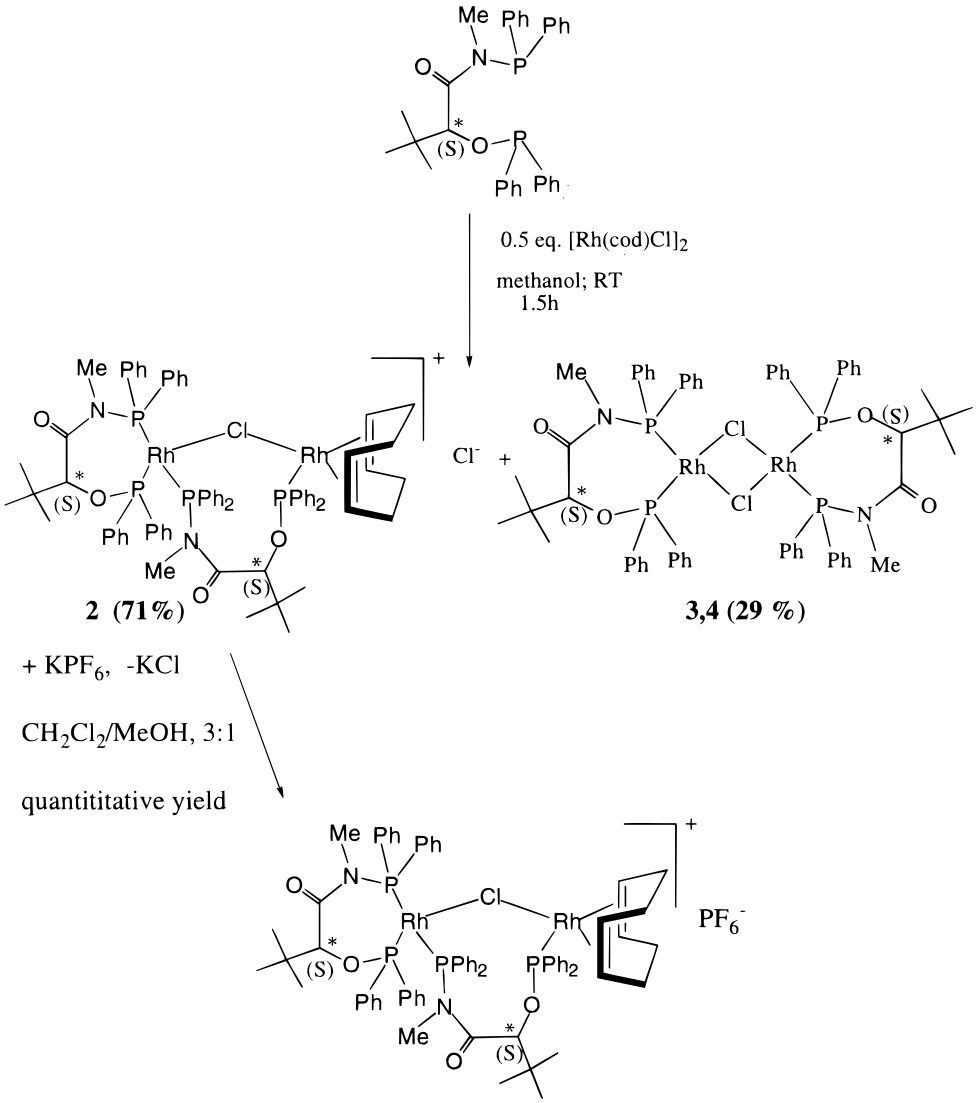

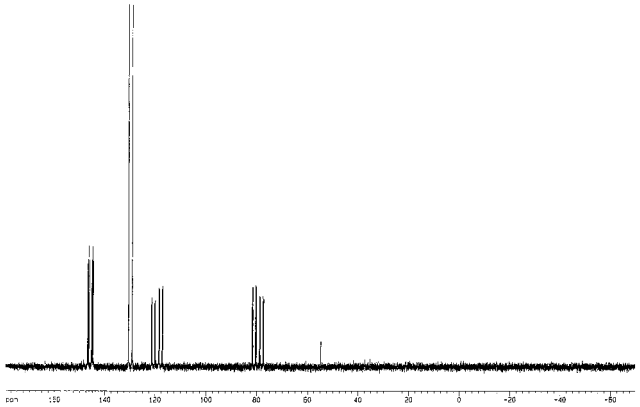

Figure 1. ^{31}P NMR spectrum of **2** showing the four nonequivalent P-donors. The two lowest frequency resonances stem from the P−N ligands and show a large ^2J(P,P) value of 354 Hz, indicative of a trans orientation of these spins (162 MHz, CD_2Cl_2).

respectively, and was isolated as both its Cl and PF_6 salts (see Scheme 1 and the Experimental Section).

A ^{31}P NMR spectrum of **2** is given in Figure 1. Of the four nonequivalent ^{31}P signals, one is a simple doublet, arising from ^{103}Rh coupling. The absence of a $^2J(^{31}P,^{31}P)$ coupling constant suggests that this is not a chelating ligand but rather a bridging moiety.

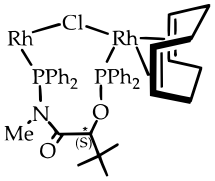

An in situ, inverse $^{103}Rh,^{31}P$-detected NMR spectrum[11,12] measured after 3 days in solution is shown in Figure 2. This spectrum reveals that (a) there are two nonequivalent ^{103}Rh spins in **2** and (b) one of these is coupled to a single ^{31}P and the second is coupled to three ^{31}P spins. The two low-frequency ^{31}P-resonances in **2** reveal a common, relatively large $^2J(^{31}P,^{31}P)$ value, 354 Hz. This

(11) Pregosin, P. S. Inorganic Nuclei: Low Sensitivity Transition Metals. In *Encyclopedia of Nuclear Magnetic Resonance*; John Wiley & Sons Ltd.: Chichester, 1996; Vol. 4.

(12) Tedesco, V.; von Philipsborn, W. *Organometallics* **1995**, *14*, 3600. Bender, B. R.; Koller, M.; Nanz, D.; von Philipsborn, W. *J. Am. Chem. Soc.* **1993**, *115*, 5889. Ernsting, J. M.; Elsevier, C. J.; de Lange, W. D. J.; Timmer, K. *Magn. Reson. Chem.* **1991**, *29*, S118. Imhof, D.; Rüegger, H.; Venanzi, L. M.; Ward, T. R. *Magn. Reson. Chem.* **1991**, *29*, 73.

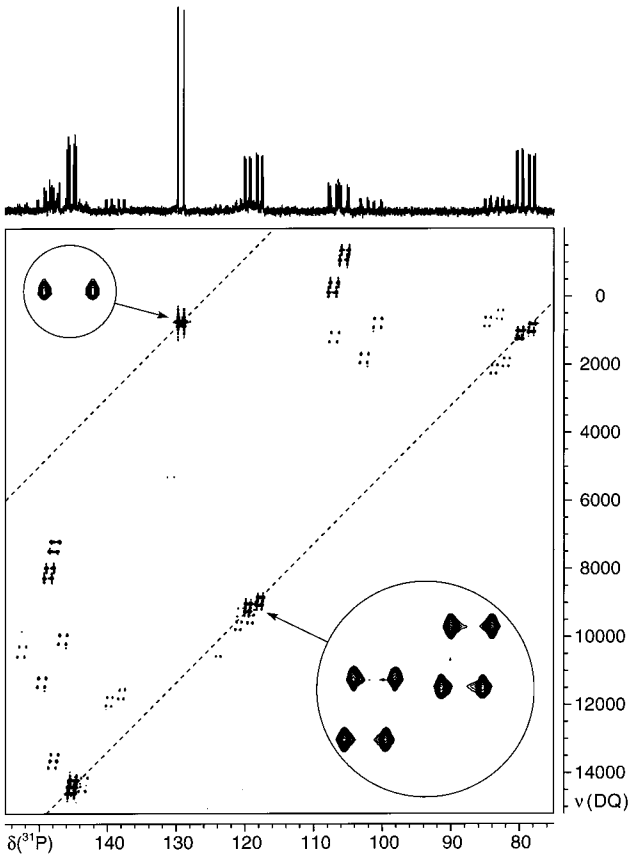

Figure 2. $^{103}Rh-^{31}P$ heteronuclear double-quantum spectrum of an aged sample of **2**, showing two ^{103}Rh chemical shifts (emphasized by dashed skew diagonals) involving one and three phosphorus resonances, respectively. The inserts exhibit the multiplicity of the rhodium signals with respect to phosphorus in the vertical dimension. The upper left insert reveals a singlet, and the lower right insert has a doublet of doublets, in accordance with AX and ABCX spin systems, respectively. The vertical splitting in the latter multiplet corresponds to the appropriate sums of passive coupling constants $^1J(^{103}Rh,^{31}P) + {}^2J(^{31}P,^{31}P)$. Note that $^2J(^{31}P,^{31}P)_{trans}$ is of the opposite sign to $^2J(^{31}P,^{31}P)_{cis}$ and $^1J(^{103}Rh,^{31}P)$. The spectrum also shows signals arising from **3** and **4** plus resonances arising from an isomer of **2**.

is consistent with nonequivalent trans P-donors.[13] On the basis of its $^2J(^{31}P,^{31}P)$ and $^1J(^{103}Rh,^{31}P)$ values, the fourth ^{31}P spin in **2** is cis to these two and trans to a weak donor.

^{13}C NMR spectroscopy[14] on **2** reveals four nonequivalent olefin signals, suggesting a coordinated 1,5-COD. Two of these signals resonate at relatively high frequency, 112.4 and 112.7 ppm, while the other two, 70.9 and 71.6 ppm ($^1J(^{103}Rh,^{13}C)$ values of 13.9 and 13.3 Hz, respectively), are much closer to the position for the four equivalent olefin carbons of $[Rh(\mu\text{-}Cl)(1,5\text{-}COD)]_2$ (δ = 79.0 ppm, $^1J(^{103}Rh,^{13}C)$ = 13.9 Hz, this work, in CD_2Cl_2, literature = 78.5 ppm[14]). The protons corresponding to the carbon signals at 70.9 and 71.6 ppm, assigned via a C,H-correlation, show NOE's to aromatic protons (presumably from the bridging P−O), whereas the protons corresponding to the carbons at 112.4 and 112.7 ppm do not show NOE's to aromatic protons. Taken together, all of these NMR results lead to the following somewhat unexpected structure:

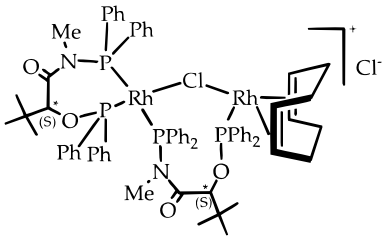

major isomer of **2**

A $^{31}P,^1H$ correlation allows the unambiguous assignment of the two P−N phosphorus types via their three-bond correlations to the N−Me groups. The same principle is valid for the P−O ^{31}P signals using the methine CHO resonances. Consequently, it is certain that a P−O donor is coordinated to the Rh atom complexing a COD moiety and that two P−N donors are mutually trans. However, the ^{103}Rh spectrum of the aged sample, in Figure 2, suggests that there are very small quantities of geometric isomers of **2**, i.e., species in which the relative positions of the P donors are different.

Interestingly, Mortreux and co-workers[15a] have recently reported that related amidophosphine−phosphinite ligands react with $[Rh(\mu\text{-}Cl)(COD)]_2$ in toluene at 25 °C to give the complexes $[Rh(\mu\text{-}Cl)(chelate)]_2$ in *15 min*! Obviously, the use of MeOH as the solvent slows the reaction markedly.

$[Rh(\mu\text{-}Cl)(Ph\text{-}t\text{-}Lanop)]_2$. Complexes **3** and **4** are the sym-trans and sym-cis forms, respectively, of the dinuclear complex [Rh(?-Cl)(**1**)]$_2$. This mixture can be

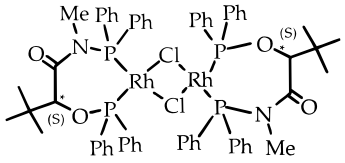

3

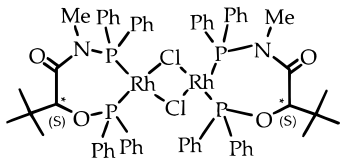

4

obtained as the methanol-isoluble fraction or by waiting several weeks for **2** to rearrange in CD_2Cl_2 solution. ^{31}P NMR data for **3** and **4** and further complexes are also given in Table 1. It is worth noting that the $^1J(^{103}Rh,^{31}P)$ values for **3** (ca. 217 Hz for the P−O and 220 Hz for the P−N) and **4** (ca. 217 Hz for the P−O and 221 Hz for the P−N) are relatively large, as expected for a ^{31}P spin trans to a μ-Cl.[15] Both ^{31}P and ^1H 2-D NOESY spectra show that **3** and **4** are in equilibrium

(13) Pregosin, P. S.; Kunz, R. W. *^{31}P and ^{13}C NMR of Transition Metal Phosphine Complexes*; Springer-Verlag: Berlin, 1979; Vol. 16.
(14) Mann, B. E.; Taylor, B. F. *^{13}C NMR Data for Organometallic Compounds*; Academic Press: London, 1981.

(15) (a) Roucoux, A.; Thieffry, L.; Carpentier, J.; Devocelle, M.; Meliet, C.; Agboussou, F.; Mortreux, A.; Welch, A. J. *Organometallics* **1996**, *15*, 2440. (b) Agboussou, F.; Carpentier, J.; Hatat, C.; Montreux, A.; Betz, P.; Goddard, R.; Krüger, C. *Organometallics* **1995**, *14*, 2480.

Table 1. ^{31}P NMR Data for the Complexes[a]

	$[Rh_2Cl(\mathbf{1})_2(1,5\text{-COD})]Cl$, **2**	$[RhCl(\mathbf{1})]_2$, **3** and **4**[b]
P(O)	nb: 145.8 (192/40, 34) b: 129.9 (179)	**3**: 147.4 (217, 41) **4**: 149.0 (217, 39, ^3J(Rh,P) = 6)
P(N)	nb: 79.6 (354, 163, 40) b: 119.3 (354, 152, 34)	**3**: 102.4 (220, 42) **4**: 100.4 (218, 39), ^3J(Rh,P) = 6)

	$[Rh_2Cl(\mathbf{1})_3]PF_6$, **6**	[Rh(COD) (**1**)]OTf, **7a**
P(O)	P2 144.6 (192, 42, 35) P4 ca. 122 (172, 355) P6 136.0 (202, 39, 44)	132.8 (167, 25)
P(N)	P1 82.2 (163, 355, 42) P3 118.6 (154, 355, 35) P5 85.5 (148, 451, 39)	84.1 (169, 25)

	[RhCl(PPh_3) (**1**)], **8**	[Rh(CO)(PPh_3)(**1**)]Cl, **9**
P(O)	145.5 (203, 32, $^2J(P_O,PPh_3)$, 38)	145.7 (202, 32; $^2J(P_O,PPh_3)$, 38)
P(N)	89.8 (159, $^2J(P_O,P_N)$, 32 ($^2J(P_N,PPh_3)$ = 392)	90.1 (159; 32; $^2J(P_N,PPh_3)$, 392)
PPh_3	37.0 (132, $^2J(P_O,PPh_3)$), 38 ($^2J(P_N,PPh_3)$, 392)	37.5 (139, $^2J(P_O,PPh_3)$, 38 ($^2J(P_N,PPh_3)$, 392)

	$[Rh(solvent)_2(\mathbf{1})]OTf$, **10**	[RhCl(tBu-NC) (**1**)], **11**[c]
P(O)	153.8 (227/57)	**I**: 145.2 (193, 35) **II**: 141.4 (147, 30)
P(N)	108.5 (229/57)	**I**: 90.7 (152, 34) **II**: 89.3 (br)

[a] Measured at room temperature in CD_2Cl_2 at 400.13 MHz for ^{1}H, 162 MHz for ^{31}P. Bridging and nonbridging **1** are denoted as b and nb, respectively. Chemical shifts are in ppm, and coupling constants, Hz, are in brackets, with ^1J(Rh,P) first followed by $^2J(P_O,P_N)$. [b] Ratio of **3**:**4** is ca. 3:1. [c] Isomer **I** has rather sharp signals at room temperature, whereas isomer **II** has more broad signals. The ratio of **I**:**II** is ca. 1:0.83.

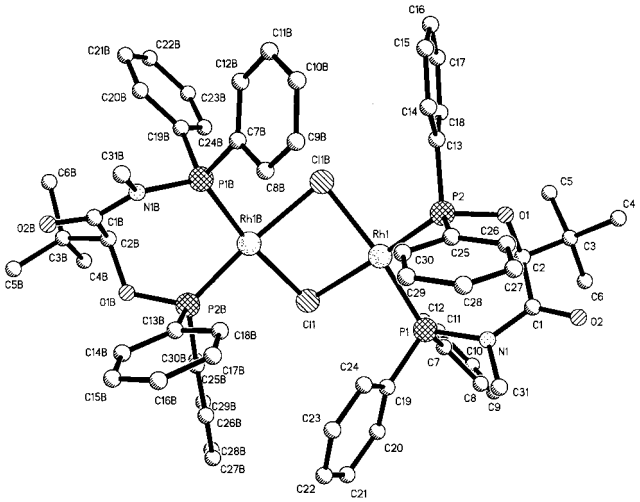

Figure 3. Plot of the structure of **3**, $[Rh(\mu\text{-}Cl)(\mathbf{1})]_2$, as the sym-trans isomer.

on the NMR time scale in CD_2Cl_2. Complex **3** (which is 3 times more abundant than **4**) crystallizes from solution, and its solid-structure was determined via X-ray diffraction, see Figure 3.

The structure of the sym-trans isomer **3** contains two pseudo-square-planar Rh(I) units sharing a common edge. There is a puckered Rh_2Cl_2 four-membered ring, as expected,[16−19] with the two Cl−Rh−Cl planes making a ca. 131° angle. The two chelating ligands are not identical. The metal−phosphorus Rh−(P−N) bond lengths (ca. 2.178(1), 2.184(1) Å) and the two Rh−(P−O) separations (ca. 2.163(1), 2.177(1) Å) are all similar, but slightly shorter than the Rh−P bond length found in $[Rh(\mu\text{-}Cl)(PPh_3)_2]_2$,[17] 2.200(2) and 2.213(2) Å. The Rh−(P−O) separations are significantly shorter than the Rh−(P−N) separations. This is normal for this type of complex,[15b] and this point will be mentioned again in connection with $[Rh(1,5\text{-COD})(\mathbf{1})]^+$, below. The two Rh−Cl separations are different and fall in the region 2.393(9)−2.420(9) Å, in agreement with the literature.[16−19] The average chelate bite angle is 93.9°. A list of selected bond lengths and bond angles is given in Table 2. The amide unit, Me−N−C═O, is flat (torsion angles of 1−2° are found, both in the two nonequivalent molecules of **3** and in the complex with 1,5-COD, described below), thus imparting rigidity to the chelate ring; however, we note that the average N−C(1) bond distance, 1.379(5) Å, is fairly long and the average C(1)−O(2) separation, 1.218(4) Å, is fairly short. There are not many structures of $[Rh(\mu\text{-}Cl)(\text{chiral bidentate phosphine})]_2$ type complexes.[15a]

Table 2. Selected Bond Length (Å) and Bond Angle (deg) Data for μ-Cl Dinuclear Complex 3

Rh(1)−P(1)	2.1782(10)	P(1B)−N(1B)	1.746(3)
Rh(1B)−P(1)	2.1841(9)	N(1)−C(1)	1.380(5)
Rh(1)−P(2)	2.1626(9)	N(1B)−C(1B)	1.378(5)
Rh(1B)−(P2)	2.1771(10)	C(1)−O(2)	1.2106(4)
Rh(1)−Cl1	2.4155(8)	C(1B)−O(2B)	1.220(4)
Rh(1B)−Cl(1B)	2.4199(9)	C(1)−C(2)	1.531(6)
Rh(1B)−Cl(1)	2.3933(8)	C(1B)−C(2B)	1.520(5)
P(1)−N(1)	1.750(3)		
P(1)−Rh−P(2)	93.35(3)	Cl(1B)−Rh−P(1)	171.42(3)
P(1B)−Rh−P(2B)	94.39(4)	Cl(1)−Rh−P1	89.0(3)
Cl(1B)−Rh−P(2)	95.11(3)	Cl(1)−Rh−P(2)	173.4(3)

Exchange Spectroscopy. An isolated sample of **2** as its chloride salt shows interesting dynamics in CD_2Cl_2, as shown by ^{1}H 2-D exchange spectroscopy.[20,21] Within **2**, the two well-resolved olefinic protons cis to the bridging P−O donor do *not* exchange with each other;[22] however, these 1,5-COD protons do exchange with the two (overlapping) olefinic 1,5-COD protons trans to the bridging P−O ligand. Further, since neither the two nonequivalent N**Me** groups nor the two methine C**H**O signals are exchanging, the dynamics are limited to the 1,5-COD moiety.

Scheme 2 shows a possible intramolecular mechanism which rationalizes these results: (a) dissociation of the

(16) Schnabel, R. C.; Roddick, D. M. *Inorg. Chem.* **1993**, *32*, 1513.
(17) Curtin, M. D.; Butler, W. M.; Greene, J. *Inorg. Chem.* **1978**, *17*, 2928.
(18) Ibers, J. A.; Snyder, R. G. *Acta Crystallogr.* **1962**, *15*, 923.
(19) Dahl, L. F.; Martell, C.; Wampler, D. L.; *J. Am. Chem. Soc.* **1961**, *83*, 1761.
(20) Hull, W. E. In *Two-Dimensional NMR Spectroscopy. Applications for Chemists and Biochemists*; VCH: New York, 1987; p 153. Ernst; R. R.*Chimia* **1987**, *41*, 323.
(21) For applications of 2-D exchange spectroscopy, see: Pregosin, P. S.; Salzmann, R. *Coord. Chem. Rev.* **1996**, *155*, 35. Albinati, A.; Eckert, J.; Pregosin, P. S.; Ruegger, H.; Salzmann, R.; Stoessel, C. *Organometallics* **1997**, *16*, 579. Barbaro, P.; Currao, A.; Herrmann, J.; Nesper, R.; Pregosin, P. S.; Salzmann, R. *Organometallics* **1996**, *15*, 1879. Barbaro, Pregosin, P. S.; Salzmann, R.; Albinati, A.; Kunz, R. W. *Organometallics* **1995**, *14*, 5160. Herrmann, J.; Pregosin, P. S.; Salzmann, R.; Albinati, A. *Organometallics* **1995**, *14*, 3311. Pregosin, P. S.; Salzmann, R.; Togni, A. *Organometallics* **1995**, *14*, 842. Breutel, C.; Pregosin, P. S.; Salzmann, R.; Togni, A. *J. Am. Chem Soc.* **1994**, *116*, 4067; *Magn. Reson. Chem.* **1994**, *32*, 297. Lianza, F.; Macchioni, A.; Pregosin, P. S.; Rüegger, H. *Inorg. Chem.* **1994**, *33*, 4999.
(22) It was conceivable that NOE between these two neighboring olefinic signals dominates the exchange signals; however, inspection of the NOE map for the CH_2 protons adjacent to these olefin resonances (which do not show strong NOE's to one another) shows that these are also clearly not in exchange, thereby negating the "swamping" idea).

Scheme 2. Intramolecular isomerization of 2

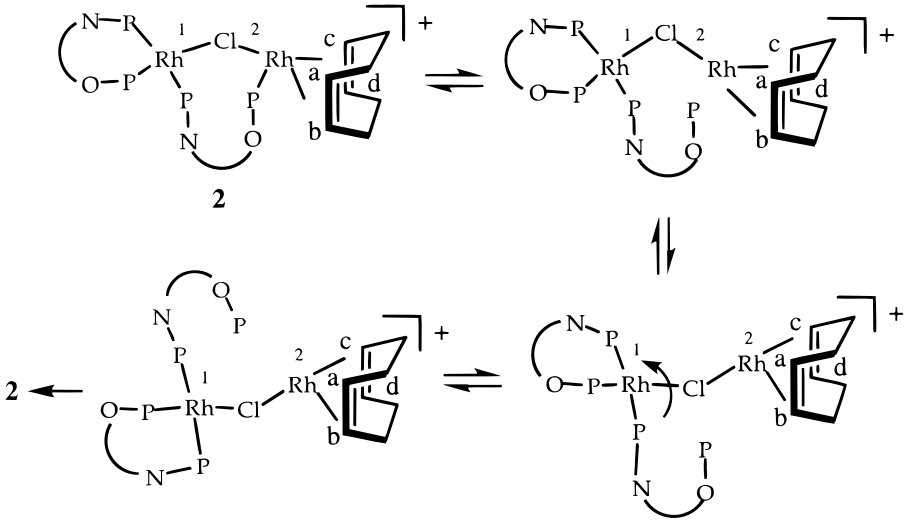

P−O donor from Rh(2) in **2**; (b) isomerization of the resulting three-coordinate complex, i.e., chloride moves from pseudo-trans to "a,b" to pseudo-trans to "c,d"; (c) rotation around the Rh(1)−Cl bond; and (d) recombination to give **2**.

In the same exchange spectrum, one finds that all four of these olefinic COD protons in **2** are in exchange with a broad proton resonance at 4.12 ppm, whose corresponding ^{13}C spectrum has a doublet at 76.6 ppm, $^1J(^{103}Rh,^{13}C) = 13.3$ Hz. These NMR data are reminiscent of but not identical to $[Rh(\mu\text{-}Cl)(COD)]_2$ (δ $^1H = 4.27$ ppm, δ $^{13}C = 79.0$ ppm, $^1J(^{103}Rh,^{13}C) = 13.9$ Hz, this work). The resonance at 4.12 cannot corespond to [Rh(1,5-COD)(**1**)]$^+$ since we have prepared this complex independently (see below). Integration in the conventional spectrum shows that the ratio of **2** to this unknown is ca. 7.5:1. As we do not observe ^{31}P signals for the unknown, we assume that these dynamics stem from an intermolecular exchange process, whose details are not clear, but which involves $[Rh(\mu\text{-}Cl)(COD)]_2$. We considered **5** as a structural possibility for the resonance at 4.12 ppm, with δ $^{13}C = 76.6$ ppm. It is an attractive

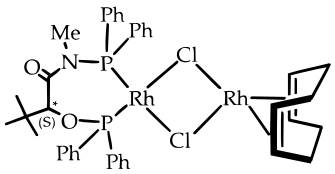

5

alternative since it is easy to envision its formation via loss of ligand **1** from **2**, followed by Cl^- addition. The reverse reaction, i.e., addition of **2** to **5**, would explain the intermolecular dynamics. However, there is no hard evidence for its existence.

After several days in CD_2Cl_2 solution, a ^{31}P 2-D exchange spectrum shows **2**−**4** present. The two complexes **3** and **4** are in equilibrium, but there is no exchange of either of these with **2**. As noted above, there is a slow reaction in CD_2Cl_2 solution which transforms **2** into **3** and **4** over several days.

^1H 2-D exchange spectroscopy in CD_2Cl_2 solution on a solution of isolated **2** as its PF_6^- salt reveals the previously recognized exchange plus new processes.[23] Both the intra- and intermolecular processes described above are, again, identifiable. This suggests that **2** does not need Cl^- for the intramolecular process. Again, neither the two nonequivalent N**Me** groups nor the two methine C**H**O of **2** are exchanging. However, there are two new broad 1,5-COD signals at δ 3.8 and 4.3 which exchange with each other but not with **2**. Regretably, one observes impurities which are also dynamic on the NMR time scale, so that a more detailed analysis was not undertaken.

Additional Complexes. It is also possible to prepare a dinuclear complex containing three complexed Ph-t-Lanop ligands, **6**, by treating the PF_6 analog of **2** with an additional equivalent of **1** in methylene chloride solution. Complex **6** was identified via its ^{31}P NMR

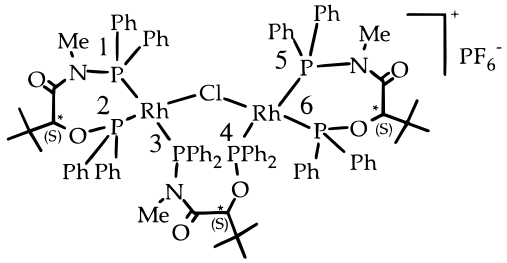

6

spectrum, ^{31}P COSY, FAB mass spectroscopy, and elemental analyses. In CD_2Cl_2, the two bridging ^{31}P spins of **6** are found fairly close together: 118.6 and ca. 122 ppm with the latter multiplet relatively broad. Since one of the three CHO methine proton signals is also broad, we assign the dynamic site to the bridging P−O donor. This is consistent with, but not proof of, the mechanism offerred in Scheme 2, i.e., P−O dissocia-

(23) The PF_6 analogue was prepared in the hope of excluding Cl^--catalyzed exchange as a mechanism. A solution of the PF_6^- compound affords the olefin compound with its 4.12 ppm signal. Moreover, in solution, the same exchange pattern is recognized; however, there are new unidentified complexes which are also involved in exchange. Further, the exchange is now somewhat slower, which could be interpreted as resulting from a decrease in the concentration of chloride present in solution. Thus, we cannot rigorously exclude Cl^- as being involved.

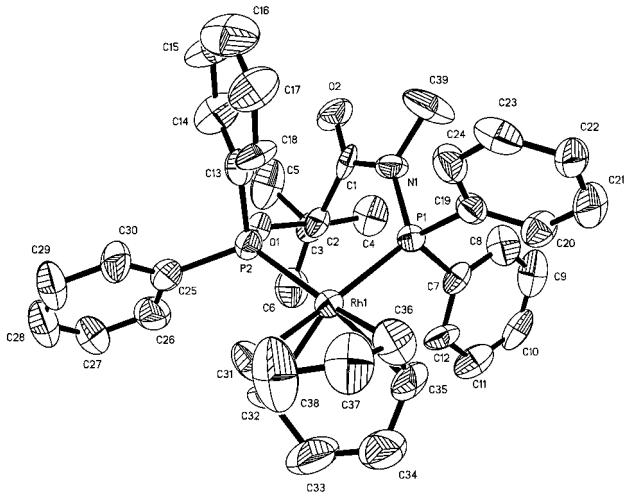

Figure 4. Plot of the structure of **7a**, [Rh(1,5-COD)(**1**)]-OTf. The view is from above and behind the diolefin.

Table 3. Bond Lengths (Å) and Bond Angles (deg) for Complex 7a

Rh−C(32)	2.220(8)	N(1)−C(39)	1.486(10)
Rh−C(31)	2.248(7)	C(1)−O(2)	1.174(8)
Rh−C(35)	2.299(7)	C(1)−C(2)	1.531(10)
Rh−C(36)	2.290(8)	C(2)−C(3)	1.537(9)
Rh−P(1)	2.3163(18)	C(2)−O(1)	1.403(7)
Rh−P(2)	2.2765(16)	O(1)−P(2)	1.636(5)
P(1)−N(1)	1.779(6)	C(31)−C(32)	1.332(12)
N(1)−C(1)	1.379(8)	C(35)−C(36)	1.408(13)
P(1)−Rh−P(2)	93.63(7)	C(32)−Rh−P(1)	156.1(2)
C(32)−Rh−P(2)	95.4(2)	C(31)−Rh−P(1)	166.9(2)
C(31)−Rh−P(2)	90.7(2)	C(36)−Rh−P(1)	94.4(2)
P(2)−Rh−C(36)	153.0(3)	C(35)−Rh−P(1)	90.1(2)
P(2)−Rh−C(35)	169.6(2)		

tion. In general, we observe that the chelating ^{31}P−O signals are found at higher frequency than the ^{31}P−N signals; however, the bridging P−O and P−N donors often had similar ^{31}P chemical shifts.

The cationic olefin complex [Rh(1,5-COD)(**1**)]$^+$ was prepared as both its OTf and BF_4 salts **7a,b**, using $[RhCl(1,5\text{-}COD)]_2$, 2 equiv of **1**, and either Ag OTf or $AgBF_4$. With the Cl^- removed, the coordination of **1** is

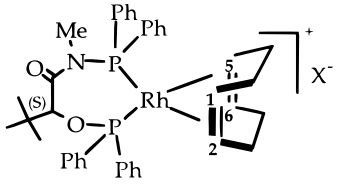

7a, X = OTf **7b,** X= BF_4

facile. The solid-state structure of **7a** was determined by X-ray diffraction, and a view of the molecule is shown in Figure 4. A list of selected bond lengths and bond angles is given in Table 3. The Rh−C(olefin) distances fall in the range ca. 2.22−2.29(8) Å, with the two metal−carbon distances trans to the P−O donor longer than those trans to the P−N donor. The Rh−P(1), 2.316(2) Å, and Rh−P(2), 2.277(6) Å, separations are as expected;[24,25] however, the Rh−P−O distance is, as noted above, considerably shorter than the Rh−P−N separation. The P−Rh−P angle is ca. 93.7°.

When viewed from behind 1,5-COD, there is a slight counterclockwise rotation of 1,5-COD with respect to the P−Rh−P plane, as indicated from the angle data shown:

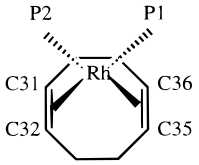

P1-Rh-C31 = 164° P2-Rh-C36 = 153°

P1-Rh-C32 = 156° P2-Rh-C35 = 170°

An angle of 180° would place the corresponding carbon in the plane.

The ^{31}P data for **7a** are given in Table 1. The olefinic ^{13}C signals, C1, C2, C5 and C6 (which correspond to C31, C32, C35, and C36 from the X-ray study), appear at δ 101.7, 98.8, 104.1, and 115.3, respectively, in the OTf complex. The assignment of these signals was made as follows: there are four well-separated ^{1}H olefin signals (δ 5.20, 4.49, 4.83, and 4.31, respectively) which can be correlated pairwise via a COSY spectrum to each other and then to the four ^{13}C resonances. A ^{31}P,^{1}H-correlation assigns the four sets of ortho P-phenyl resonances, which, in turn, via NOE's, allows a distinction between H1,H2 and H5,H6. Within the two pairs, the assignment is less certain and is based on the relative intensities of cross peaks in the NOE map. In any case, there is a considerable spread in these ^{13}C chemical shifts. We do note that there is some correlation of the ^{13}C olefin chemical shifts with the observed Rh−C(olefin) bond lengths in that the highest frequencies are associated with the longest distances, i.e., the carbons trans to the P−O donor appear at the highest frequencies. We consider this trend to be an expression of the differing electronic capabilities of these two phosphorus donors.

The PPh_3 complex **8** (see Scheme 3) was prepared from $RhCl(PPh_3)_3$ and **1**. Its ^{31}P P−N resonance at 89.8 ppm and the PPh_3 signal at 37.0 ppm both show the characteristically large $^2J(^{31}P,^{31}P)$ coupling constant, 392 Hz, associated with a trans orientation of these spins, thus assigning the correct geometry. The ^{31}P P−O signal appears at 145.5 ppm. A similar NMR approach was used to assign the correct geometry for **9**, which was prepared from $RhCl(CO)(PPh_3)_2$ and **1**. On the basis of **2**, **8**, and **9**, it would appear that the P−O donor prefers to be trans to the weaker Cl-type ligand when the alternative is a phosphorus donor. The reaction of the cation [Rh(1,5-COD)(Ph-t-Lanop)]OTf with 1 atm of hydrogen at ambient temperature in MeOH afforded an air-sensitive cationic solvento complex, **10**. Although isolable, we had difficulty in obtaining analytical data for **10** and give its ^{31}P NMR data (MeOH-d_4) in Table 1. As is often the case,[24,25] one cannot be certain as to whether water, triflate, or methanol (or some mixture of these) take up the remaining coordination positions. We find no indication for hydride complexes.

The t-Bu isonitrile complex RhCl(t-BuNC)(**1**), **11**, was prepared from **3** with 2 equiv of t-BuNC and exists in

(24) Stang, P. J.; Cao, D. H.; Poulter, G. T.; Arif, A. M. *Organometallics* **1995**, *14*, 1110.

(25) Schmülling, M.; Grove, D. M.; van Koten, G.; van Eldik, R.; Veldman, N.; Spek. A. L. *Organometallics* **1996**, *15*, 1384.

Scheme 3

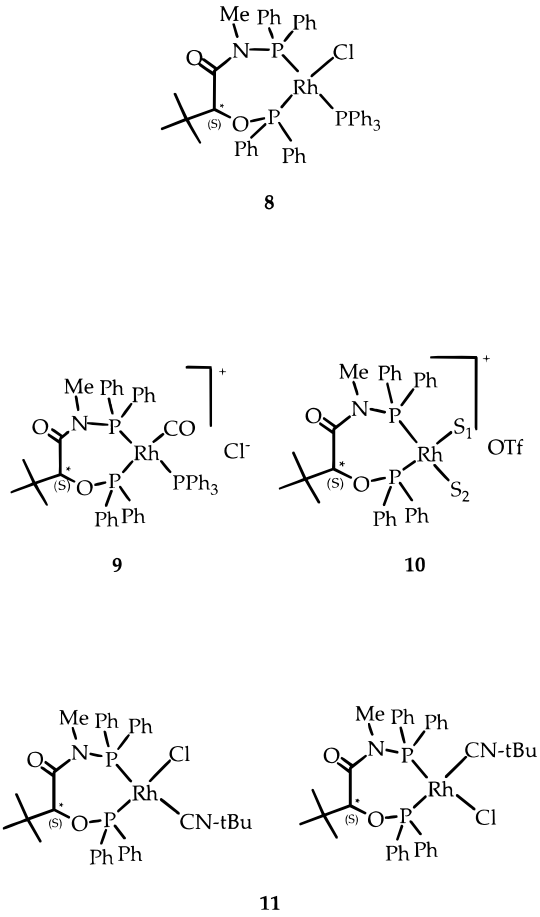

the two geometric forms shown in Scheme 3. The major isomer shows relatively sharp ^{31}P resonances, whereas the P−N donor for the minor isomer is quite broad. These isomers are in equilibrium, as shown by the ^{1}H NMR exchange spectrum in Figure 5.

This exchange is slow but relatively rapid compared to that described for the equilibrium between **2** and **5**, as witnessed by the considerable line broadening. It is noteworthy that the methine OCH resonance reveals both three- and four-bond $^{31}P,^{1}H$ coupling constants. This is a characteristic of all of the complexes which contain chelating (but not bridging) **1**. A summary of selected ^{1}H and ^{13}C NMR data for the complexes is given in Table 4.

At ambient temperature, the isomers of **11** are found in the ratio ca. 1:0.8, whereas at 253K (at which temperature the ^{31}P NMR lines are all sharp), the rato is ca. 2:1. NOE and $^{31}P,^{1}H$-correlation data at ambient temperature suggest that the major isomer has the nitrile cis to the P−O donor; however, relative to **2**, **8**, and **9**, the structural preference is not so marked. From complexes **7**−**11**, it is clear that **1** coordinates smoothly to Rh(I) in a variety of environments.

Conclusions

A series of Rh(I) complexes (including several dinuclear derivatives with bridging **1**) containing Ph-t-LANOP are readily prepared. The P−O and not the P−N phosphorus donor seems to exercise the largest trans influence, as suggested by both X-ray crystallography and NMR spectroscopy.

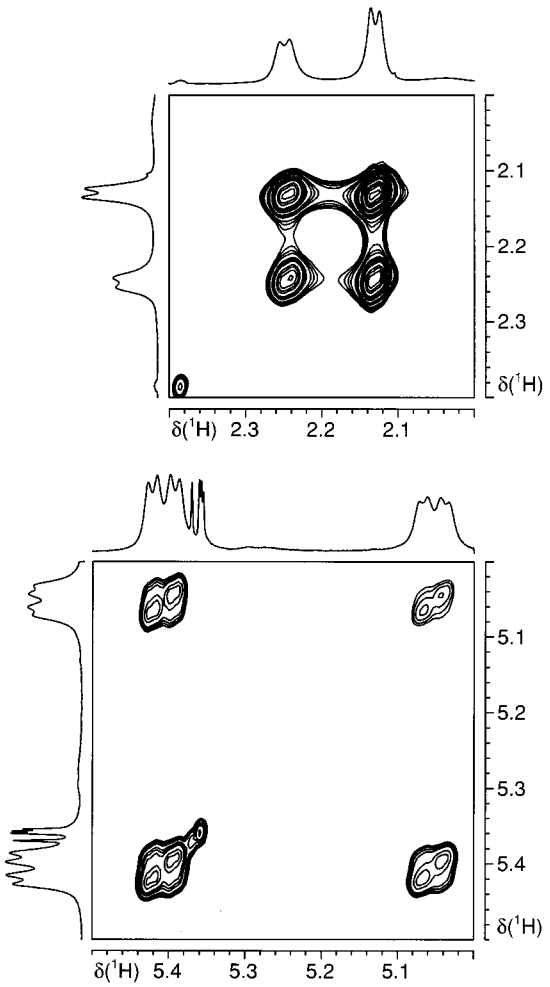

Figure 5. Two sections of the ambient-temperature NOESY spectrum of RhCl(t-BuNC)(**1**), **11**. The upper trace shows the N−Me region, and the lower trace shows the methine CHO region. There are two geometric isomers, with the minor species having slightly larger line widths. Note that both of the methine C**H**O protons show three- and four-bond coupling constants to ^{31}P (400 MHz, CD_2Cl_2).

Experimental Section

General. All reactions were performed in an atmosphere of Ar using standard Schlenk techniques. Dry and oxygen-free solvents were used. (*S*)-Ph-t-LANOP and $[Rh(1,5\text{-COD})Cl]_2$ were kindly provided by Hoffman-La Roche AG, Basel. Routine ^{1}H, ^{31}P, and ^{13}C NMR spectra were recorded with Bruker DPX-250, DPX-300, DRX-400, and AMX-500 spectrometers. Chemical shifts are given in ppm, and coupling constants (*J*) are given in hertz. 2-D NMR spectra were measured as reported previously.[21] For the NOESY measurements, a mixing time of 0.8 s was employed. IR spectra were recorded with a Perkin-Elmer 882 infrared spectrophotometer. Elemental analyses were performed by the Micoanalytical laboratory of the ETH. Mass spectra were carried out at the Mass Spectroscopy Service of the ETH.

X-ray Crystallographic Studies. Intensity data for **3** were collected at 243 K on a STOE IPDS (image plate detector system). An absorption correction (ψ scan) was performed

Table 4. Selected ^{1}H and ^{13}C NMR Data[a] for the Complexes

complex	CH−O[b]	NMe
2	5.32, (10.8/5.6) nb	1.95 nb
	82.8 nb	32.7 nb
	6.17b	2.90 b
	78.3 b	35.3 b
3	5.29 (10.5/4.3)	1.90 (5.7)
	82.4 (10.3/1.8)	33.3
4	5.18 (10.1/4.8)	1.76 (6.0)
	81.9 (11.2)	33.4
7a[b]	5.18 (10.5/5.0)	2.34 (5.8)
	84.8 (10.2/1.4)	34.4 (2.4)
8	5.60 (10.3/5.4)	2.10 (4.8)
	81.3 (12.8/1.6)	33.9
9	5.60 (10.3/5.4)	2.09 (4.8)
10	5.19 (10.0/4.3)	2.03 (6.4)
	84.1 (10.1)	33.9
11, major	5.41 (11.8/4.8)	2.13 (4.7)
	82.9 (12.6)	33.8
11, minor	5.05 (11.4/4.3)	2.25 (5.3)
	85.2 (10.5)	33.9

[a] Chemical shifts in ppm, and P,H coupling constants, in parentheses, in hertz, CD_2Cl_2 solutions. nb = chelating; b = bridging. ^{13}C data immediately below the ^{1}H data. [b] The larger of the two ^{31}P coupling constants arises from ^3J(P,H). [c] 1,5-COD olefin NMR data in the text.

Table 5. Experimental Data for the X-ray Diffraction Study of 3 and 7

	3	**7**
formula	$C_{62}H_{66}Cl_2N_2O_2O_4P_4Rh_2$	$C_{40}H_{45}F_3NO_{7.75}P_2RhS$
temperature	243(2) K	293(2) K
radiation	Mo Kα graphite monochromated	
cryst syst	orthorhombic	monoclinic
space group	$P2_12_12_1$	$P2_1$
a, Å	14.816(1)	9.8169(7)
b, Å	16.192(1)	14.6983(13)
c, Å	25.553(1)	30.141(3)
α, deg	90	90
β, deg	90	90.56(3)
γ, deg	90	90
V, Å^3	6130.2(6)	4348.8(6)
Z	4	2
ρ, calcd, g cm^{-3}	1.413	1.402
μ, mm^{-1}	0.776	0.575
cryst dimens, mm	0.23 × 0.68 × 0.38	0.72 × 0.63 × 0.36
data collection	STOE IPDS	STOE STADI 4
θ range, deg	$4.02 \le \theta \le 24.09$	$1.54 \le \theta \le 22.49$
no. of indep data collected	9616 [$^aR_{int} = 0.0362$]	5936
data/restr/params	9616/0/685	5906/15/1208
$^bR_1$ ($I > 2\sigma(I)$)	0.0261	0.0465
$^cR_2$ ($I > 2\sigma(I)$)	0.0617	0.1318
$^bR_1$ (all data)	0.0291	0.0897
$^cwR_2$ (all data)	0.0631	0.1987
^{d}Goof on F^2	1.053	1.093

[a] $R_{int} = \sum|F_o^2 - F_o^2(\text{mean})|/\sum[F_o^2]$. [b] $R_1 = \sum||F_o| - |F_c||/\sum|F_o|$. [c] $wR_2 = \{\sum[w(F_o^2 - F_c^2)^2]/\sum[w(F_o^2)^2]\}^{1/2}$. [d] GooF = $\{\sum[w(F_o^2 - F_c^2)^2]/(n-p)\}^{1/2}$ (n = no. of reflections, p = no. of parameters refined); $w = 1/[\sigma^2(F_o^2) + (aP)^2 + bP]$, $P = [2F_c^2 + \text{Max}(F_0^2,0)]/3)$.

with DECAY.[26] Details of this and the following structure determination are given in Table 5.

Intensity data for **7** were collected on an STOE STADI4 four-circle diffractometer at room temperature. An empirical absorption correction (ψ scan) was performed. The occurrence of weak superstructure reflections required a doubling of the c-axis to 30.141 Å. With respect to the cation of **7**, the crystal structure shows an almost perfect translational symmetry with one-half the lattice constant along the crystallographic c-axis. Only the arrangement of the triflate counterions requires a description with the doubled c-axis and, therefore, gives rise to the weak superstructure reflections. Several disordered solvent molecules were found and described with 5.5 equiv of oxygen per formula unit.

For **3** and **7**, the structure solution (direct methods) refinement with full-matrix least squares on F^2 plus the molecular graphics, the Siemens program package SHELXTL Version 5 was used.[27] All non-hydrogen atoms were refined with anisotropic thermal displacement parameters, and all hydrogen atoms were placed at their calculated positions and refined (riding model) with different isotropic thermal displacement parameters for each group.

Synthesis of [Rh$_2$(μ-Cl)((*S*)-Ph−t-LANOP)$_2$(1,5-COD)]-Cl, 2, and [Rh(μ-Cl)((*S*)-Ph−t-LANOP)]$_2$, 3 and 4. To a solution of 108.7 mg (0.212 mmol) of (*S*)-t-LANOP in 4 mL of methanol was added 0.50 equiv (52.2 mg; 0.106 mmol) of [Rh(μ-Cl)(1,5-COD)]$_2$. After 90 min, the precipitate which appeared was washed once with 2 mL of MeOH, filtered, and dried in vacuo to afford a yellow powder. Yield: 40.0 mg (29%). The filtrate was evaporated to dryness and produced an orange powder. yield: 106 mg (71%). MS (FAB): found 1375.0 (M$^+$), 1144.9, 1128.9; calcd 1376.6. IR (CsI): 1668 cm^{-1} (C═O of PP ligand). Anal. Calcd for $C_{70}H_{78}N_2O_4P_4Rh_2Cl_2$: 59.54 (C), 5.57 (H), 1.98 (N). Found: 58.88 (C), 5.37 (H), 1.90 (N). **B**: MS (FAB): found 1302.4 (M); calcd 1303.9. Anal. Calcd for $C_{62}H_{66}N_2O_4P_2Rh_2Cl_2$: 57.12 (C), 5.10 (H), 2.15 (N). Found: 56.54 (C), 5.11 (H), 2.07 (N).

Synthesis of [Rh$_2$(μ-Cl)((*S*)-Ph-t-LANOP)$_2$(1,5-COD)]-PF$_6$. A mixture of 40.1 mg (0.0284 mmol) of [((*S*)-t-LANOP)$_2$Rh$_2$-(1,5-COD)Cl]Cl, **2**, and 50 mg of KPF_6 (9.6 equiv, 0.27 mmol) was stirred for 10 min in 5 mL of CH_2Cl_2/methanol (ca. 3/1). After evaporation to dryness, the crude product was extracted with 10 mL of CH_2Cl_2. Filtration of the extract and subsequent drying in vacuo gave 43 mg (100%) of a yellow powder. MS (FAB): found 1375.1 (M$^+$); calcd 1376.6. IR (CsI): 1684 (C═O of nonbridging PP ligand), 1551 (C═O of bridging PP ligand), 839 cm^{-1} (PF_6). Anal. Calcd for $C_{70}H_{78}N_2O_4P_5Rh_2$-$ClF_6$: 55.26 (C), 5.17 (H), 1.84 (N). Found: 55.00 (C), 5.23 (H), 1.70 (N).

Synthesis of [Rh$_2$(μ-Cl)((*S*)-Ph-t-LANOP)$_3$]PF$_6$, 6. A solution of **2** (24.6 mg, 0.0162 mmol) and **1** (8.30 mg, 0.0162 mmol) in 2 mL of CH_2Cl_2 was stirred at room temperature for 3 h, and the resulting solution was evaporated to dryness. Washing with hexane to remove **1** afforded 29 mg (93%) of a yellow powder. MS (FAB): found 1783 (M$^+$); calcd 1782. Anal. Calcd for $C_{93}H_{99}ClF_6N_3O_6P_7Rh_2$: 57.97 (C), 5.18 (H), 2.18 (N). Found: 58.84 (C), 5.431 (H), 2.12 (N).

Synthesis of [Rh((*S*)-Ph-t-LANOP)(1,5-COD)]OTf, 7a. A mixture of 65.3 mg (0.127 mmol) of (*S*)-Ph-t-LANOP, 0.50 equiv (31.3 mg; 0.0636 mmol) of [Rh(μ-Cl)(1,5-COD)]$_2$, and 1 equiv (32.7 mg, 0.127 mmol) of AgOTf in 3 mL of CH_2Cl_2 was stirred for 1 h. Subsequently, the reaction mixture was filtered over Celite and evaporated to dryness. The solid material was then washed with 3 mL of THF, followed by washing twice with 2 mL of hexane. This affords the product as a yellow powder: yield, 105 mg (95%). MS (FAB): found 724.3 (M$^+$); calcd 724.7. IR (KBr): 1682 (C═O of PP ligand), 1262 cm^{-1} (OTf). Anal. Calcd for $C_{40}H_{45}F_3NO_5P_2SRh$: 54.99 (C), 5.19 (H), 1.60 (N). Found: 54.76 (C), 5.28 (H), 1.67 (N).

Synthesis of [Rh((*S*)-Ph-t-LANOP)(1,5-COD)]BF$_4$, 7b. A mixture of 70.8 mg (0.144 mmol) of [Rh(1,5-COD)Cl]$_2$ and 2.1 equiv (59.0 mg, 0.303 mmol) of $AgBF_4$ in 15 mL of CH_2Cl_2 was stirred for 30 min at room temperature. After filtration, 2.0 equiv (147.5 mg, 0.287 mmol) of (*S*)-Ph-t-LANOP was added. After 5 min, the solution was filtered over Celite and then evaporated to dryness to afford 221 mg (95%) of a yellow powder. MS (FAB): found 724.7 (M$^+$); calcd 724.1. IR (KBr): 1675 (C═O of PP ligand), 1154−994 (BF_4). Anal. Calcd for

(26) *STOE IPDS program package, Version 2.81*; Stoe & Cie: Darmstadt.

(27) *SHELXTL Version 5*; Siemens Analytical X-ray Systems, Inc.: Madison, WI.

$C_{39}H_{45}BF_4NO_2P_2Rh$: 57.73 (C), 5.59 (H), 1.73 (N). Found: 57.71 (C), 5.48 (H), 1.88 (N).

Synthesis of RhCl((*S*)-Ph-t-LANOP)(PPh_3), 8. A suspension of 101.0 mg (0.109 mmol) of $RhCl(PPh_3)_3$ and 1.0 equiv (56.1 mg. 0.109 mmol) of (*S*)Ph-t-LANOP was stirred in dry acetone for 2 days. Evaporation to dryness gave a brown tar. The crude material was washed twice with 10 mL of hexane. Subsequently, the crude product was disolved in 8 mL of dry acetone and filtered. Evaporation to dryness resulted in 90 mg (90%) of product as a yellow powder. MS (FAB): found 913.1 (M) and 878.2 (M^+); calcd 914.3 and 878.8. IR (CsI): 1668 (C═O of PP ligand), 251 cm^{-1} (Rh−Cl). Anal. Calcd for $C_{49}H_{48}NO_2P_3RhCl$: 64.38 (C), 5.29 (H), 1.53 (N). Found: 65.28 (C), 5.21 (H), 1.02 (N).

Synthesis of [Rh((*S*)-Ph-t-LANOP)(CO)(PPh_3)]Cl, 9. A solution of 32.8 mg (0.0475 mmol) of $RhCl(CO)(PPh_3)_2$ and 1.0 equiv (24.4 mg, 0.0475 mmol) of (*S*)-Ph-t-LANOP in 2 mL of CH_2Cl_2 was stirred for 30 min and then evaporated to dryness. Washing twice with 10 mL of hexane and drying in vacuo gave 42 mg (93%) of a yellow powder. IR (CsI): 1965 (Rh−CO), 1670 cm^{-1} (C═O of PP ligand). Anal. Calcd for $C_{50}H_{48}NO_3P_3$-RhCl: 63.74 (C), 5.13 (H), 1.49 (N). Found: 63.52 (C), 5.23 (H), 1.33 (N). The complex is a 1:1 electrolyte based on conductivity measurements.

Synthesis of [Rh((*S*)-Ph-t-LANOP)(solvent)$_2$]OTf, 10. A solution of 14.0 mg of [(*S*)-Rh(Ph-t-LANOP)(1,5-COD)]OTf in 2 mL of methanol was stirred in an atmosphere of H_2 overnight. After evaporation to dryness, the crude product was washed with hexane to remove the organic products and then dried in vacuo to afford an air-sensitive yellow powder. It is not certain whether the complex contains coordinated MeOH. Water and/or triflate are also possibilities.[24,25] Its ^{31}P NMR spectrum was measured in MeOH-d_4.

Synthesis of RhCl((*S*)-Ph-t-LANOP)(t-Bu-NC), 11. To a solution of 21.5 mg (0.0165 mmol) of [Rh(μ-Cl)((*S*)-t-LANOP)]$_2$ in 2 mL of CH_2Cl_2 was added 2 equiv (3.7 mL, 0.033 mmol) of *tert*-butyl isocyanide. The solution became instantaneously yellow. After 5 min, the reaction mixture was evaporated to dryness, washed with hexane, and then dried to afford 24 mg (100%) of a yellow powder. MS (FAB): found 782.3 ((PP)Ru(t-Bu-NC)$_2$), 699.2 (M^+); calcd 699.6. IR (CsI): 2187 (NC of t-Bu−NC), 1674 (C═O of PP ligand), 200 cm^{-1} (Rh−Cl). Anal. Calcd for $C_{36}H_{42}N_2O_2P_2RhCl$: 58.83 (C), 5.76 (H), 3.81 (N). Found: 58.26 (C), 5.77 (H), 4.36 (N).

Acknowledgment. P.S.P. thanks the Swiss National Science Foundation, the ETH Zurich, and F. Hoffmann-La Roche AG, Basel, for financial support. We also thank F. Hoffmann-La Roche AG, Basel, for the gift of the Lanop bidentate ligand as well as Johnson Matthey for the loan of $RhCl_3$. Special thanks are due Dr. Heinz Rüegger for the ^{103}Rh spectrum and Dr. M. Wörle for the X-ray structures.

Supporting Information Available: Tables of crystal data, atomic coordinates, bond lengths, bond angles, anisotropic displacement parameters, and hydrogen coordinates for **3** and **7a** (21 pages). Ordering information is given on any current masthead page.

OM9802008